RSC Advances

ROYAL SOCIETY OF CHEMISTRY

www.rsc.org/advances

RSC Advances

RSCPublishing

ARTICLE

Superior CO_2 Adsorption from Waste Coffee Ground Derived Carbons

Cite this: DOI: 10.1039/x0xx00000x

Will Travis, Srinivas Gadipelli and Zhengxiao Guo*

Received 00th January 2012,
Accepted 00th January 2012

DOI: 10.1039/x0xx00000x

www.rsc.org/

Utilising the hugely abundant waste from spent coffee grounds (CGs), KOH activated highly microporous carbons with surface areas of 2785 m^2/g and micropore volumes of 0.793 cm^3/g were synthesised that are capable of uptake capacities near 3 mmol/g at 50 °C and 1 bar. Importantly such uptake capacities are achieved though the material's superior microporous character and without doping within the carbon matrix, thereby ensuring facile regeneration with a binding enthalpy of only 26 kJ/mol and therefore capable of energy unintensive cycleable adsorption processes. Furthermore, excellent tunability of pore-size is demonstrated from narrow micropores through to narrow mesopores, enabling optimised adsorption over a range of pressures.

1. Introduction

The increasing level of atmospheric carbon dioxide (CO_2) from anthropogenic emissions is arguably the greatest scientific concern of modern times. Of these emissions 80% are a result of coal, oil and natural gas combustion.[1] An effective method for CO_2 capture and sequestration (CCS) from industrial point sources is therefore in urgent demand. Conventional methods for CO_2 capture utilise aqueous liquid amines but these are hindered by high regeneration energy consumption, equipment corrosion and toxicity. Increasingly, microporous solids such as metal organic frameworks (MOFs), porous carbons, zeolites and porous organic polymers (POPs) have shown varied potentials as solution to the problem of industrial CO_2 capture.[2-4] Within these materials the CO_2 uptake capacities of porous carbon such as zeolite templated carbon FAU-ZTC and carbon molecular sieve VR-93 are comparable with any other high performing solid sorbents at elevated pressures, without the high synthesis costs and instability found in many MOFs and POPs.[2, 5-7] While sorbents such as lithium silicates are capable sorbents at high temperatures.[8] At ambient conditions the narrow microporosity found in porous carbons such as polyacrylonitrile derived ACM-5 (activated carbon monolith)[9] and carbide-derived carbons[10] mean their CO_2 capacities are equal to any microporous solid thus far reported. Within the field of porous carbon the use of KOH as an activating agent has produced materials with remarkable porous properties from a wide variety of precursors.[11-16] Some of these materials achieve CO_2 uptakes of >4 mmol/g at 25 °C and 1 bar, among the highest achieved for porous solids and outperforming current commercial activated carbons such as Maxsorb, BPL and Norit R1 (Table S1). For the production of activated carbons as CO_2 sorbents it is understood that the careful selection of carbon precursor has a profound impact on the resultant performance where success is determined by economic cost and final CO_2 capacity among other factors such as energy of regeneration. Table S1 highlights various precursors that have been commonly utilised to synthesise the very best performing activated carbons, such as: polymers, hard-templated mesoporous carbons and biomass.[4, 9, 12, 17-21] From an industrial viewpoint an ideal precursor must not only deliver a high-performing sorbent, but also be highly abundant and capable of carbon yields suitable for extensive mass production. Coffee is considered the second largest traded commodity in the world,[22] and as such spent coffee grounds (CGs) represent a tremendously abundant precursor to activated carbon. This high abundance makes them extremely attractive relative to the other commonly utilised precursors presented in Table SI, while the resultant sorbents which are discussed in this paper show capacities well in excess of current commercial activated carbons[23-25]. It has been highlighted that to compete with existing liquid amine technology, solid sorbents will need to achieve a working capacity of ~3 mmol CO_2/g sorbent at ≥50 °C and ambient flue pressures.[26] To achieve this N-doping has frequently been used to enhance uptake at elevated temperatures. However, this increase in adsorbate-adsorbent interaction results in an increased cost of regeneration and a trade-off between high micropore character and nitrogen content may be desirable. In this paper we report that from moderate KOH activation of waste CGs we obtain a porous

carbon sorbent with CO_2 uptake among the best sorbents at ambient conditions and elevated temperatures. We highlight the importance of successful sorbents to achieve a working capacity of ~3 mmol CO_2/g sorbent at ≥50 °C, and show that this can be achieved at 1 bar CO_2 using an undoped highly microporous CG derived carbon with low enthalpies of adsorption and therefore facile regeneration. We also stress that reports often omit performance at such elevated temperatures and few meet such stringent requirements.[6, 7, 9, 10, 26]

2. Experimental

2.1. Synthesis

We have synthesised a series of KOH activated carbons from spent coffee grounds. Wet fresh grounds of Starbucks Dark Roast coffee were removed from a DeLonghi ECAM 23.450.S machine and dried in a vacuum oven for 24 h at 120 °C obtaining dry grounds (CG). These dry grounds were then heated at either 400 or 700 °C under N_2 to carbonise to chars and remove volatiles present in the grounds. This was carried out by charging a ceramic crucible with CG and then loading this into a Lenton horizontal wire wound tube furnace, heating at 3 °C/min to the desired temperature, dwelling for 2 h. The furnace was purged with N_2 for 30 min before heating and N_2 flowed throughout heating. These samples have been labelled CGx, where x denotes the thermal treatment temperature. Following char formation chemical activation was carried out by grinding KOH with the CGx using a pestle and mortar until a fine grey mixture was achieved. Using the tube furnace activation was carried out at 700 °C, heating at 3 °C/min and dwelling for 1 h, the tube was N_2 purged and N_2 flowed throughout. The solid black carbon product was then washed with distilled water until washes with a neutral pH achieved and the resulting black carbon vacuum oven dried at 120 °C. Ratios of 2-1 and 4-1 KOH-CGx were used.

2.2. Sample Characterisation

Low-temperature nitrogen adsorption-desorption isotherms were measured at 77 K using a Quantachrome Autosorb-IQ2 machine. Specific surface area was measured using the desorption isotherm within relative pressures of 0.01 and 0.2, in accordance with the Brunauer-Emmett-Teller (BET) method. Quenched Solid Density Functional Theory (QSDFT) assuming slit and cylindrical pores was used to measure micro- and mesopore volumes. Total pore volume was estimated from the amount of nitrogen adsorbed at a relative pressure of 0.99. CO_2 adsorption isotherms at 0-1 bar were also measured on the IQ2 at 273, 298 and 323 K. The high-pressure CO_2 adsorption-desorption isotherms at 0-10 bar were measured at 273 and 298 K, using a Hy-Energy PCTPro-2000. X-ray photoemission spectroscopy (XPS) was carried out using a Thermo Scientific Al-K-alpha. Thermogravimetric analysis (TGA) was carried out using a Setaram Setsys 16/18 machine. Scanning electron microscopy (SEM) was performed using a Jeol JSM-6301F microscope. X-ray diffraction (XRD) was performed using a Bruker axs, D4 endeavor with Cu-K-alpha radiation.

3. Results and Discussion

3.1. Sample Analysis

The CGs were initially dried and then converted into 'char' via pyrolysis in inert atmosphere. This CG char formation step has been shown crucial for successful KOH activation.[22] Figure S1 shows thermogravimetric analysis (TGA) for the pyrolysis (Argon atmosphere, rate 2 °C/min) of the CGs to form the CG char. The weight loss at 200-400 °C can be ascribed to degradation of the lignocellulosic materials into heavier hydrocarbons (tars) and gaseous products such as H_2O, CO, CO_2, CH_4 and aldehydes.[27] Evolution of the heavier hydrocarbons is expected to to occur up to 500 °C and the weight loss observed at 600-700 °C is known to be from char consolidation.[22] From understanding of this pyrolysis process we formed chars with and without char consolidation, via thermal treatments at 400 and 700 °C respectively. It is understood that the degradation of the lignocellulosic material is required before activation to afford a highly microporous solid.[22] We obtained CG 400 and CG 700 with weight loss of 70 and 74 % respectively, Table S2 shows the yields obtained for CGx and the activated products achieved relative to the amount of dry grounds initially used. Chemical activation was carried out on the CG chars using ratios of 2:1 and 4:1 KOH:CGx by weight. Sample yields ranged from 11 to 16 wt.% with yields lower for higher KOH concentrations. As yields of 15 % are typical for commercial activated carbons the industrialized scale up of this synthesis appears reasonable on this basis.[28, 29] The highest yield was achieved for a 2:1 ratio of KOH:CG 400, the burn-off (percentage of weight loss for chars after chemical activation process) was 47 %, meaning a yield of 16 % from dry CG starting material to the activated carbon product. From SEM analysis we show that particulate sizes of the activated CGs are in the 5-30 μm range and as such are normal for activated carbons touted for industrial applications (Figure S2). [5, 30-32]

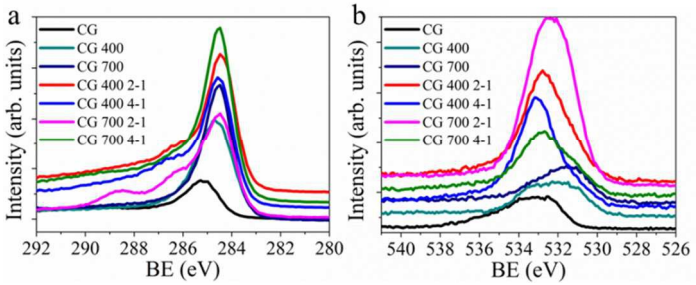

Figure 1. XPS analysis (a) C 1s spectra and (b) O 1s Spectra.

The structural impact of the KOH activation can be observed from the XRD pattern (Figure S3). The CGs indicate some short-range order with a broad peak around 20° 2θ, attributed to aromatic stacking of the cellulosic forms, following pyrolysation graphitic type domains are apparent with broad peaks at 20-25° 2θ for the CG chars. This broad peak is shifted to higher 2θ values for CG 700, closer to ordered graphite at 26.5°, indicating a greater degree of graphitisation. For the activated samples this graphitic-order is reduced due to the

etching and pore formation processes. Pore formation is also indicated by broadening in the low angle scatter up to higher 2θ values for the activated CGs relative to the CG chars and this is attributed to an increase in the density of pores following activation.[13] XPS elementary analysis (Figure S4 and Table S2) shows that the CG carbons consist of carbon and oxygen atoms only, no nitrogen is present and all activating potassium ions have been removed in the washing process. The absence of nitrogen is noteworthy as nitrogen-dopants have been widely touted to increase carbon based sorbents' enthalpies of CO_2 sorption.[33] The two dominant peaks at binding energies (BE) of 284.5 and 533.0 eV represent C 1s and O 1s environments respectively (Figure 1, a and b respectively). The C 1s peaks at 284.5 eV indicate the carbon species are predominately in graphitic-type C=C systems,[34] the O 1s broad peaks at 532.5-533.5 eV can be expected to be phenolic-type OH groups.[35, 36] From Table S2 we see that the KOH activated samples possess typically higher oxygen at.% than the CG chars. This can also be seen in the C 1s spectra for activated species where features at 288-286 eV are indicative of carbon in an oxygen bound environment. The O 1s peak of CG 700 at 531.5 eV is indicative of C=O functionality, this peak shifts to 532.5-533.5 eV which may be interpreted as phenolic –OH functionality resulting from KOH treatment or adsorbed surface H_2O.[36, 37] The porous structure of the materials has been evaluated using nitrogen adsorption and desorption isotherms at 77 K (Figure 2a). The surface areas have been calculated using the BET method and shown in Table 1. The two samples with KOH:CGx ratios of 2:1 show highly microporous structures with type-I adsorption curves. The steep increase in the adsorption curve at low relative pressures is indicative of a developed narrow microporosity. The samples with higher KOH:CGx ratios of 4:1 show a more hierarchical pore architecture. A high degree of microporosity, in conjunction with this developed narrow mesoporosity can be observed from a wider knee in the adsorption isotherm. Analysis of cumulative pore volume (Figure S5) and pore size distribution (Figure 2b) using a quenched solid DFT (QSDFT) which quantitatively accounts for the surface roughness, shows that for both CG 400 2-1 and CG 700 2-1, more than 90 % of porosity is centred below 1.5 nm.

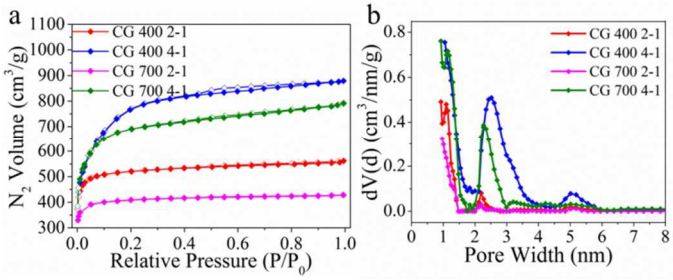

Figure 2. (a) Nitrogen adsorption (solid) and desorption (open) isotherm for KOH activated CGs at 77 K. (b) Corresponding pore size distribution plots

Table 1. Porous properties for the CG-derived carbon

Material	SSA_{BET} (m^2/g)	V_P (cm^3/g)	V_{micro} (cm^3/g)	Pore width (nm)
CG 400 2-1	2073	0.869	0.731	0.926
CG 400 4-1	2785	1.36	0.716	1.051
CG 700 2-1	1624	0.662	0.589	0.966
CG 700 4-1	2620	1.225	0.793	0.926

SSA_{BET} (Specific Surface Area BET) was calculated in the partial pressure (P/P_0) range of 0.01-0.1. Total pore volume (V_p) measured at P/P_0 = 0.99. Microporous pore volume (V_{micro}) for pores less than 2 nm determined from nitrogen sorption using the QSDFT method assuming slit and cylindrical pores. Pore width is the micropore width (mode) calculated from the QSDFT method.

In turn, in the samples with higher KOH:CGx ratios of 4:1 we observe pore opening in narrow mesopores of 2-4 nm in width as well as in micropores. During activation potassium metal ions (or carbon bound adducts thereof) become incorporated within the carbon matrix, and subsequent decomposition of carbonate leads to disorder and pore formation.[14] This developed narrow mesoporosity for samples with greater KOH concentration can be ascribed to a greater degree of carbon burn-off upon the potassium reduction that creates larger porous architectures.

3.2. CO_2 Uptake Performance

The CO_2 adsorption-desorption isotherms measured at 0 and 25 °C and 0-10 bar are shown in Figure 3, with adsorption isotherms at 0-1 bar inset. The desorption curves show no hysteresis, indicating that adsorption is fully reversible. Adsorption capacities at 1 and 10 bar for the samples are shown in Table 2, and show excellent adsorption in the low and high pressure region. At low pressures (1 bar CO_2) CG 700 2-1, with a pore structure principally consisting of narrow micropores with a micropore volume of 0.589 cm^3/g, shows high adsorption at 1 bar CO_2 (7.17 mmol/g at 0 °C and 4.21 mmol/g at 25 °C), and as such is comparable to the very best porous solid materials thus far reported, see Table S1 and references therein. We show pore sizes can be controlled by changing the KOH concentration, obtaining narrow mesoporosity when the higher concentration of 4:1 KOH:CGx is used (Figure 2b). As this higher KOH concentration opens up more porosity, increasing surface area and total pore volume, the 4:1 KOH:CGs show enhanced uptake at elevated pressure; CG400 4-1 and CG 700 4-1 both show high uptakes of >23 mmol/g at 10 bar and 0 °C. These values are again among the best porous carbons reported at this time.[5, 7, 25, 38] Thus the CG derived carbons are high performing CO_2 sorbents suitable for low and high pressure applications from an abundant CG biomass.

Table 2. CO_2 capacities for the CG-derived carbon

Material	CO_2 uptake at 1 bar (mmol/g)			CO_2 uptake at 10 bar (mmol/g)	
	0 °C	25 °C	50 °C	0 °C	25 °C
CG 400 2-1	7.17	4.21	2.47	16.44	12.74
CG 400 4-1	5.09	2.81	1.52	23.27	16.05
CG 700 2-1	7.55	4.42	2.86	13.34	11.59
CG 700 4-1	6.89	4.00	2.38	23.26	16.81

Many high performing porous carbon sorbents are synthesised through use of activating agents (CO_2, KOH, K_2CO_3), with a variety of different carbon sources. Carbon precursors prepared by hard-template approaches using sacrificial zeolites are widely reported, as too are a range of polymers, usually containing high benzene content and sometimes by soft template processes. These approaches may be hindered for industrial applications as they require etching for removal of zeolite template, time consuming curing stages, are subjective to low yields and complex polymer synthetic methods.[11] That an abundant waste biomass can be utilised as precursor and deliver capacities competitive with any other porous carbon solid is of paramount importance, particularly as current commercial activated carbons are also synthesised using similar abundant materials but have lower uptake capacities. Maxsorb, a petroleum pitch derived KOH activated carbon, Norit R1 an activated carbon derived from peat and the coconut husk derived activated carbon A, all show uptakes of ~2 mmol/g at 25 °C and 1 bar, compared to the 4.4 mmol/g for CG 700 2-1.[23-25 39] At low pressure the CO_2 capacity of these carbons is also superior to most MOFs and modified MOF structures being >1.3 mmol/g (0.15 bar and 25 °C) (Table S3).[40-42]

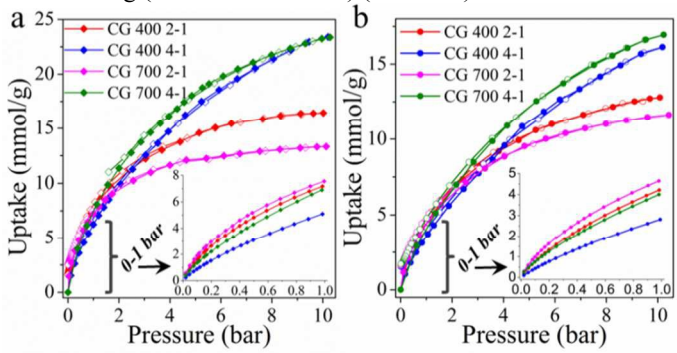

Figure 3. CO_2 adsorption (solid) and desorption (open). (a) 0 °C and (b) 25 °C, 0-10 bar: inset, adsorption isotherms up to 1 bar for KOH activated CG-derived carbons.

Materials' CO_2 uptakes at ≥50 °C are of notable import for post-combustion capture applications, yet are frequently omitted in literature. The performance of solid carbon sorbents where reported is shown in Table S3 and indicates that the CG derived carbons are among the most capable sorbents at this temperature. CG 700 2-1 achieves a CO_2 capacity of 2.86 mmol/g at a 0-1 bar pressure swing and 50 °C (Figure 4a), as shown this is comparable with other highly microporous materials. However, such materials are still some way from the target of approaching or better that 3 mmol/g at 50 °C, from a flue gas at 1.015 bar and of 15 % CO_2.[26] To increase uptake at elevated temperatures many porous carbons contain N-dopants, increasing the adsorbent-adsorbate interaction energy. However, such materials will therefore incur a greater energy penalty for regeneration. The adsorbate-adsorbent interaction can be measured using CO_2 uptake measurements at 0, 25 and 50 °C. The adsorption curves at 0, 25 and 50 °C were fitted with the Hill-Langmuir model and the isosteric heats of adsorption calculated using the Clausius-Clapeyron equation. The enthalpies of adsorption (Figure S6) are typical for undoped carbon sorbents adsorbing CO_2 via a simple physisorption process, lying between 22-26 kJ/mol.[43] A 10 cycle temperature-swing process carried out under a dynamic CO_2 flow at 1 bar with adsorption at 25 °C is shown in Figure 4b and indicates no loss of performance over this time span. A relatively low temperature of regeneration (100 °C) is used.

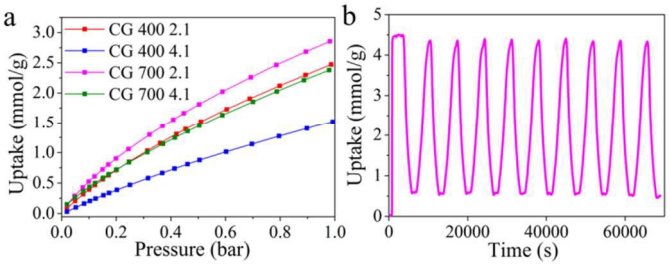

Figure 4. (a) CO_2 adsorption at isotherms at 50 °C up to 1 bar for KOH activated CG-derived carbons. (b) CO_2 adsorption-desorption cycles for CG 700 2:1 at 25 °C; regeneration achieved at 100 °C under dynamic CO_2 flow.

It is understood that micropores are principally responsible for CO_2 uptake at low pressure,[10] and therefore of interest that the 2-1 activated samples, which do not have larger micropore volumes as elucidated from nitrogen isotherms and QSDFT analysis, show greater CO_2 uptake at low pressures (Figure 3, inset). In conjunction with this is that CG 400 2-1 has greater micropore volume compared to the CG 700 2-1, yet shows lower CO_2 adsorption. While CO_2 uptakes do typically correlate with materials' micropore volumes, the deviation from correlation here is understood to be due to kinetic and pore-filling effects of the N_2 probe gas molecules at 77K when the measurements for micropore volumes are made; the N_2 probe gas molecules are effectively "blind" to ultramicropores of <0.7 nm in diameter.[44]

4. Conclusions

In conclusion, coffee grounds, highly abundant waste materials, have been transformed into an effective porous carbon sorbent material by means of char formation and controlled activation with KOH. We have demonstrated control of micro- and meso-pore distributions, achieving enhanced surface areas and total pore volumes though use of greater KOH concentrations. Notable CO_2 adsorption is achieved up to 4.4 mmol/g at 298 K

and 1 bar, and 23.3 mmol/g at 273 K and 10 bar, which are among the very best porous solid physisorbent materials as yet discovered and promise cyclical adsorption performance.

5. Acknowledgements

This work was funded by the EPSRC (EP/J020745/1; EP/G063176/1).

6. Notes and references

Department of Chemistry, University College London. 20 Gordon Street. London. WC1H 0AJ, UK.

*Email: z.x.guo@ucl.ac.uk

Electronic Supplementary Information (ESI) available: Synthesis methodology, TGA, XRD XPS, SEM, QSDFT and heats of adsorptions. See DOI: 10.1039/c000000x/

1. R. Quadrelli and S. Peterson, *Energ Policy*, 2007, **35**, 5938.
2. A. R. Millward and O. M. Yaghi, *J Am Chem Soc*, 2005, **127**, 17998.
3. D. A. Yang, H. Y. Cho, J. Kim, S. T. Yang and W. S. Ahn, *Energ Environ Sci*, 2012, **5**, 6465.
4. Z. J. Zhang, Y. G. Zhao, Q. H. Gong, Z. Li and J. Li, *Chem Commun*, 2013, **49**, 653.
5. S. Builes, T. Roussel, C. M. Ghimbeu, J. Parmentier, R. Gadiou, C. Vix-Guterl and L. F. Vega, *Phys Chem Chem Phys*, 2011, **13**, 16063.
6. J. Silvestre-Albero, A. Wahby, A. Sepulveda-Escribano, M. Martinez-Escandell, K. Kaneko and F. Rodriguez-Reinoso, *Chem Commun*, 2011, **47**, 6840.
7. H. Furukawa and O. M. Yaghi, *J Am Chem Soc*, 2009, **131**, 8875.
8. P. V. Subha, B. N. Nair, P. Hareesh, A. P. Mohamed, T. Yamaguchi, K. G. K. Warrier and U. S. Hareesh, *Journal of Materials Chemistry A*, 2014, **2**, 12792.
9. M. Nandi, K. Okada, A. Dutta, A. Bhaumik, J. Maruyama, D. Derks and H. Uyama, *Chem Commun*, 2012, **48**, 10283.
10. V. Presser, J. McDonough, S. H. Yeon and Y. Gogotsi, *Energ Environ Sci*, 2011, **4**, 3059.
11. Y. Q. Li, T. Ben, B. Y. Zhang, Y. Fu and S. L. Qiu, *Sci Rep-Uk*, 2013, **3**.
12. M. Sevilla, C. Falco, M. M. Titirici and A. B. Fuertes, *Rsc Adv*, 2012, **2**, 12792.
13. Y. W. Zhu, S. Murali, M. D. Stoller, K. J. Ganesh, W. W. Cai, P. J. Ferreira, A. Pirkle, R. M. Wallace, K. A. Cychosz, M. Thommes, D. Su, E. A. Stach and R. S. Ruoff, *Science*, 2011, **332**, 1537.
14. J. Diaz-Teran, D. M. Nevskaia, J. L. G. Fierro, A. J. Lopez-Peinado and A. Jerez, *Micropor Mesopor Mat*, 2003, **60**, 173.
15. G. Srinivas, J. Burress and T. Yildirim, *Energ Environ Sci*, 2012, **5**, 6453.
16. J. C. Wang and S. Kaskel, *Journal of Materials Chemistry*, 2012, **22**, 23710.
17. Y. Zhao, L. Zhao, K. X. Yao, Y. Yang, Q. Zhang and Y. Han, *Journal of Materials Chemistry*, 2012, **22**, 19726.
18. Y. D. Xia, R. Mokaya, G. S. Walker and Y. Q. Zhu, *Adv Energy Mater*, 2011, **1**, 678.
19. N. P. Wickramaratne and M. Jaroniec, *Acs Appl Mater Inter*, 2013, **5**, 1849.
20. D. Lee, C. Zhang, C. Wei, B. L. Ashfeld and H. Gao, *Journal of Materials Chemistry A*, 2013, **1**, 14862.
21. M. Sevilla and A. B. Fuertes, *Energ Environ Sci*, 2011, **4**, 1765.
22. A. S. González, M. G. Plaza, J. J. Pis, F. Rubiera and C. Pevida, *Energy Procedia*, 2013, **37**, 134.
23. J. P. Marco-Lozar, J. Juan-Juan, F. Suarez-Garcia, D. Cazorla-Amoros and A. Linares-Solano, *Int J Hydrogen Energ*, 2012, **37**, 2370.
24. S. Himeno, T. Komatsu and S. Fujita, *J Chem Eng Data*, 2005, **50**, 369.
25. G. Srinivas, V. Krungleviciute, Z. X. Guo and T. Yildirim, *Energ Environ Sci*, 2014, **7**, 335.
26. T. C. Drage, C. E. Snape, L. A. Stevens, J. Wood, J. W. Wang, A. I. Cooper, R. Dawson, X. Guo, C. Satterley and R. Irons, *Journal of Materials Chemistry*, 2012, **22**, 2815.
27. Z. H. Hu, M. P. Srinivasan and Y. M. Ni, *Carbon*, 2001, **39**, 877.
28. D. Kalderis, S. Bethanis, P. Paraskeva and E. Diamadopoulos, *Bioresource Technol*, 2008, **99**, 6809.
29. A. Ahmadpour and D. D. Do, *Carbon*, 1997, **35**, 1723.
30. X. Q. Fan, L. X. Zhang, G. B. Zhang, Z. Shu and J. L. Shi, *Carbon*, 2013, **61**, 423.
31. T. Tay, S. Ucar and S. Karagoz, *J Hazard Mater*, 2009, **165**, 481.
32. X. Shao, Z. Feng, R. Xue, C. Ma, W. Wang, X. Peng and D. Cao, *AIChE Journal*, 2011, **57**, 3042.
33. M. J. Zhong, S. Natesakhawat, J. P. Baltrus, D. Luebke, H. Nulwala, K. Matyjaszewski and T. Kowalewski, *Chem Commun*, 2012, **48**, 11516.
34. P. Wu, Y. D. Qian, P. Du, H. Zhang and C. X. Cai, *Journal of Materials Chemistry*, 2012, **22**, 6402.
35. Z. Y. Lin, G. Waller, Y. Liu, M. L. Liu and C. P. Wong, *Adv Energy Mater*, 2012, **2**, 884.
36. R. Larciprete, S. Fabris, T. Sun, P. Lacovig, A. Baraldi and S. Lizzit, *J Am Chem Soc*, 2011, **133**, 17315.
37. A. O. Yazaydin, R. Q. Snurr, T. H. Park, K. Koh, J. Liu, M. D. LeVan, A. I. Benin, P. Jakubczak, M. Lanuza, D. B. Galloway, J. J. Low and R. R. Willis, *J Am Chem Soc*, 2009, **131**, 18198.
38. J. Kim, S. T. Yang, S. B. Choi, J. Sim, J. Kim and W. S. Ahn, *Journal of Materials Chemistry*, 2011, **21**, 3070.
39. T. Otowa, R. Tanibata and M. Itoh, *Gas Separation & Purification*, 1993, **7**, 241.
40. S. Gadipelli, W. Travis, W. Zhou and Z. X. Guo, *Energ Environ Sci*, 2014, **7**, 2232.
41. Z. S. Zhang, J. Zhou, W. Xing, Q. Z. Xue, Z. F. Yan, S. P. Zhuo and S. Z. Qiao, *Phys Chem Chem Phys*, 2013, **15**, 2523.
42. D. M. D'Alessandro, B. Smit and J. R. Long, *Angew Chem Int Edit*, 2010, **49**, 6058.
43. B. Guo, L. Chang and K. Xie, *Journal of Natural Gas Chemistry*, 2006, **15**, 223.
44. J. Garrido, A. Linares-Solano, J. M. Martin-Martinez, M. Molina-Sabio, F. Rodriguez-Reinoso and R. Torregrosa, *Langmuir*, 1987, **3**, 76.